

Carbon Based Coatings Deposited on Nitrided Stainless Steel: Study of Thermal Degradation

Eugenia L. Dalibón, Naureen Ghafoor, Lina Rogström,
Vladimir J. Trava-Airoldi, Magnus Odén and Sonia P. Brühl

Abstract Amorphous hydrogenated carbon (DLC) coatings have a high hardness depending on the relative amount of sp^3/sp^2 bondings. They also exhibit an extremely low friction coefficient and are chemically inert. However, these coatings have some disadvantages which limit their applications. For instance, adhesion is poor when they are deposited on metallic substrates and they are also unstable at high temperatures, degrading into graphite and losing hardness. In this work, DLC coatings were deposited on precipitation hardening stainless steel (PH Corrax) which was plasma nitrided before the coating deposition. The samples were submitted to annealing treatments for an hour at different temperatures from 200 to 600 °C, together with a control group, which was only coated but not nitrided. After each annealing cycle, Raman Spectroscopy, nanoindentation and microscopy were used to check film properties. It was demonstrated that the nitriding pre treatment improved not only adhesion but also the thermal stability of the DLC, slowing degradation and preventing delamination.

E.L. Dalibón · S.P. Brühl (✉)
Surface Engineering Group, Universidad Tecnológica Nacional
(UTN-FRCU), Ing. Pereira 676, E3264BTD Concepción del Uruguay, Argentina
e-mail: sonia@frcu.utn.edu.ar; sbruhl@gmail.com

E.L. Dalibón
e-mail: dalibone@frcu.utn.edu.ar

N. Ghafoor · L. Rogström · M. Odén
Nanostructured Materials, Department of Physics, Chemistry and Biology (IFM),
Linköping University, 581 83 Linköping, Sweden
e-mail: naugh@ifm.liu.se

L. Rogström
e-mail: linro@ifm.liu.se

M. Odén
e-mail: magod@ifm.liu.se

V.J. Trava-Airoldi
Instituto Nacional de Pesquisas Espaciais (INPE), Av. dos Astronautas 1758,
12.227-010 São José dos Campos, SP, Brazil
e-mail: vladimir@las.inpe.br

Keywords DLC films · Thermal degradation · Duplex treatment · Plasma nitriding

Introduction

The DLC coatings are characterized by high hardness, low friction coefficient, good wear resistance and chemical inertia. They are used in different industrial applications such as tool coating or mechanical parts that can reach high temperatures during operation. They are frequently used for various sliding situations where they can be exposed to localized heating caused by friction, such as engine components. For these reasons, thermal stability is a very important property for different applications of DLC coatings [1, 2].

Some studies have been published about the thermal stability of DLC coatings in which it was reported that the DLC films could not retain their diamond-like properties at high temperature. This was due to the changes in their structure, because of the conversion from sp^3 bonds to sp^2 bonds [1, 3].

In order to improve the thermal stability of these coatings, either dopant elements such as Si or N or nanoparticles-dispersed composites have been added [2, 4, 5].

Another disadvantage of these films is that they present adhesion problems when they are deposited on metallic substrates. Among other reasons, this is because the carbon diffuses into the metal delaying the DLC nucleation. In addition, the iron has a catalytic effect that leads to the formation of graphite and finally, the thermal expansion coefficients of the coatings and the steels are not compatible, causing poor adhesion and high residual stresses [6].

In order to overcome these problems different interlayers between the substrate and the DLC film (e.g. Si) have been studied as well as diffusion treatments on the substrate, like plasma nitriding [6–8].

This work deals with the thermal stability of DLC coatings deposited on a particular stainless steel, the precipitation hardening type (PH), over nitrided and non nitrided substrate.

Experimental

Corrax[®] PH (Uddeholm) precipitation hardening stainless steel was used as base material. The samples were 6 mm high and 24 mm in diameter. The chemical composition in mass percentage of Corrax[®] is 0.03% C, 12% Cr, 1.4% Mo, 0.3% Mn, 0.3% Si, 9.2% Ni, 1.6% Al and Fe as balance. All samples were aged at 530 °C for 2 h according to supplier recommendations to increase hardness. Nitriding was carried out for 10 h in an industrial facility at 390 °C using a gas mixture composed of 20% N₂ and 80% H₂. The DLC coatings were deposited by the Plasma Assisted Chemical Vapor Deposition technique (PACVD) with an

asymmetrical bipolar DC pulsed discharge, using methane as the precursor gas. The process lasted 2 h and it was at 150 °C. Previously, a thin amorphous silicon interlayer was deposited using silane gas as precursor.

The DLC coatings were deposited on only aged PH stainless steel (named coated samples) and on nitrided steel (named duplex samples).

The annealing was carried out at 200, 300, 400, 500, 600 °C for 1 h on coated and duplex samples in vacuum following a method already reported in the literature [3]. The nanohardness of the films was measured employing a nano-indenter with 15 mN load before and after the annealing process.

The coatings were characterized by EDS and Raman spectroscopy before and after the thermal process as well. The microstructure of coating was analyzed by OM and SEM-FIB. The surface of coatings was observed by OM after annealing.

Results and Discussion

Microstructure of DLC Films and the Nitrided Layers

The Raman spectra for DLC coating on duplex and coated samples without annealing presented two overlapping bands known as the D and G. The D band appeared approximately at 1389 cm^{-1} and the G band, approximately at 1550 cm^{-1} . The intensity ratio of the D and G bands, I_D/I_G , was about 0.8 (Fig. 1) which indicates a low percent of sp^3 C–C bonds.

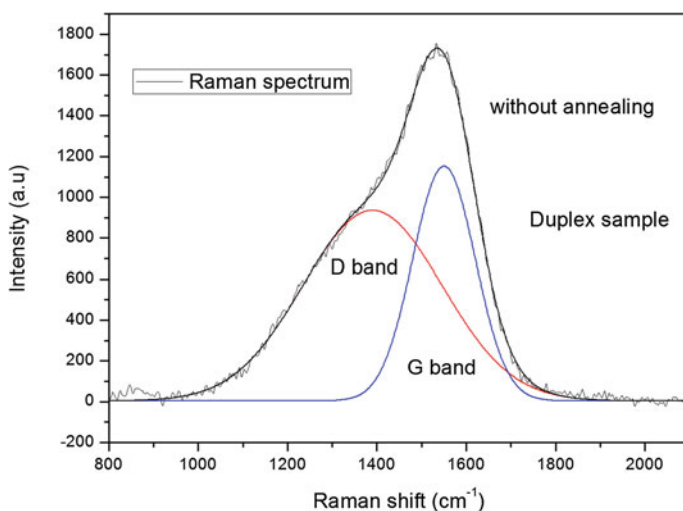
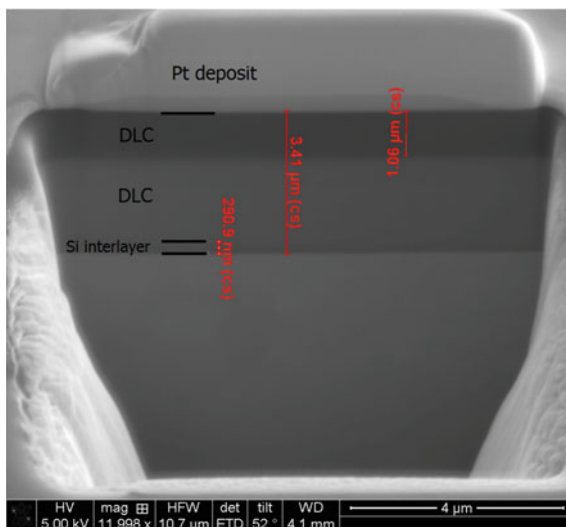


Fig. 1 Raman spectrum of duplex sample without annealing

Fig. 2 SEM image of coating on duplex sample



Moreover, according to the I_D/I_G ratio and the Full Width at Half Maximum (FWHM) of the D band, it could be inferred that the coating is largely amorphous with a cluster size smaller than 2 nm [9, 10].

The hydrogen content was about 12%, which was estimated from the slope of the fitted line to the base of the original spectrum [10].

In the EDS spectrum (not shown), C and Si were detected as expected. The coating thickness was about 3.5 μm with a two layers structure, as it can be observed in the cross-section (Fig. 2) which was analyzed by SEM/FIB. Prior to the milling process, a platinum protective layer was deposited onto the region of interest in order to prevent the erosion of the surface by the ion beam. In a previous work, the two DLC layers were analyzed and it was found that the closest layer to the surface is rich in carbon rather than silicon. The pure silicon interlayer cannot be well distinguished but it is approximately 0.3 μm. So, the EDS Si signal corresponds to the interlayer and the deeper DLC layer. The coating presented a well-defined interface with the substrate both in the duplex sample and the coated one.

The nitrated layer thickness was about 14 μm, which corresponds to a region of nitrogen in solid solution. It looked white after etching with Vilella reagent in the optical micrograph (Fig. 3). Dark regions were not observed, which normally indicates chromium nitrides precipitation and the formation of second phases.

Moreover, the XRD analysis on the duplex sample revealed α_N and γ_N peaks that correspond to nitrogen supersaturated martensite (expanded martensite) and expanded austenite respectively. There was no sign of Fe or Cr nitrides as it was reported by some of the authors on a prior publication [11].

Fig. 3 Optical micrograph of the nitrided layer

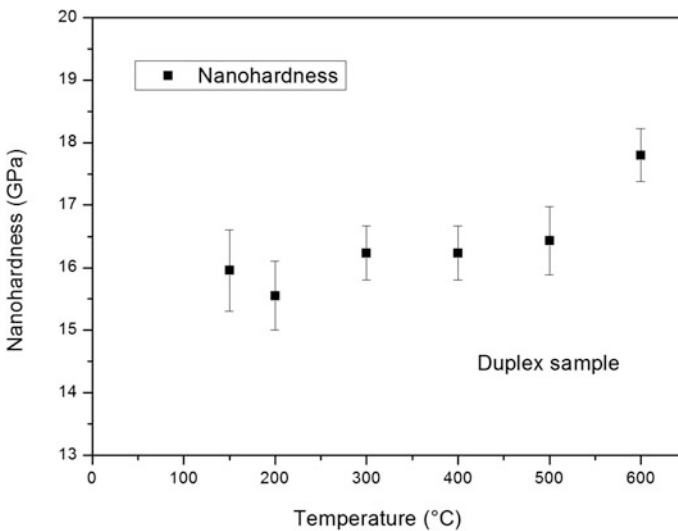
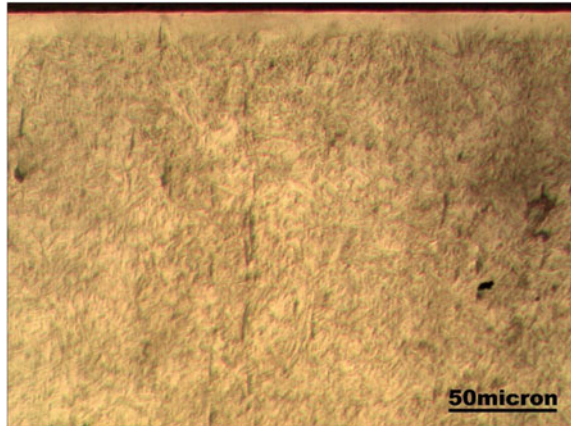


Fig. 4 Relation between nanohardness and annealing temperature of DLC coating (duplex sample)

Characterization of Coatings After Annealing

The hardness was about 16 GPa for duplex and coated samples before annealing. The results of nanohardness after the annealing and as-deposited (PACVD, 150 °C) of the duplex sample are presented in Fig. 4. Each point is the average of twenty measurements and the error was determined using the standard deviation. The hardness values obtained in both samples correspond purely to the coating hardness, because the penetration depth was less than 1/10 of the film thickness.

In the duplex sample, it can be observed that the nanohardness did not decrease; on the contrary, it remained approximately constant until 500 °C, because the variation of the hardness values is within error. At 600 °C, the hardness changed probably due to the modification of structure and morphology that the coating suffered, as it is shown below.

The results of nanohardness after the annealing and as-deposited (150 °C) of the coated sample are shown in Fig. 5.

In the coated sample, the hardness decreased at 300 °C. At 600 °C, it was not possible to obtain a value for the nanohardness because the dispersion was very large. This could be due to different factors. On one hand the coating detached in several regions (as it will be shown below) and on the other hand it is probable that the coating was transformed in some areas because of some of the hardness values were very low as it was reported in the literature for graphitization in DLC films [3]. In addition, although the hardness was measured in an area where the coating was present, the indentation could have been influenced by an adjacent uncoated area, due to the fact that plastic deformation is induced around it.

Regarding the film structure, in both samples, the Raman spectra presented similar features after annealing at different temperatures as it can be observed in Figs. 6 and 7. In order to compare both figures and show clearly the difference between spectra, the scale is the same on the “y” axis for both figures. Therefore, in the duplex sample graph (Fig. 7), the Raman spectrum corresponding to the annealing temperature of 400 °C does not appear because its background was very high and it is outside the range.

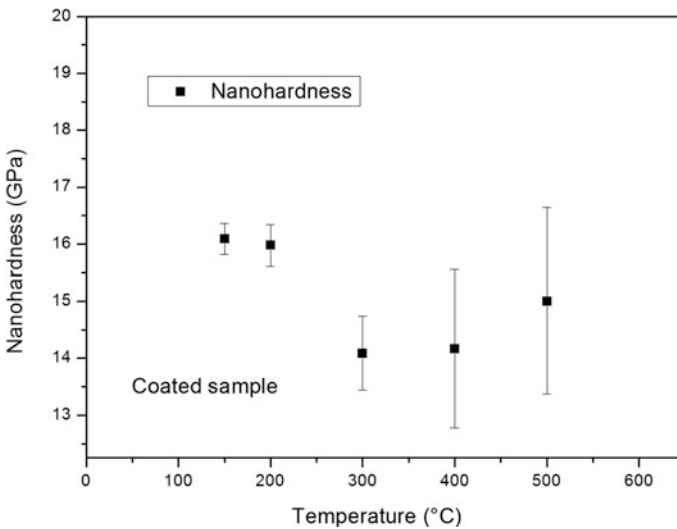


Fig. 5 Relation between nanohardness and annealing temperature of DLC coating (coated sample)

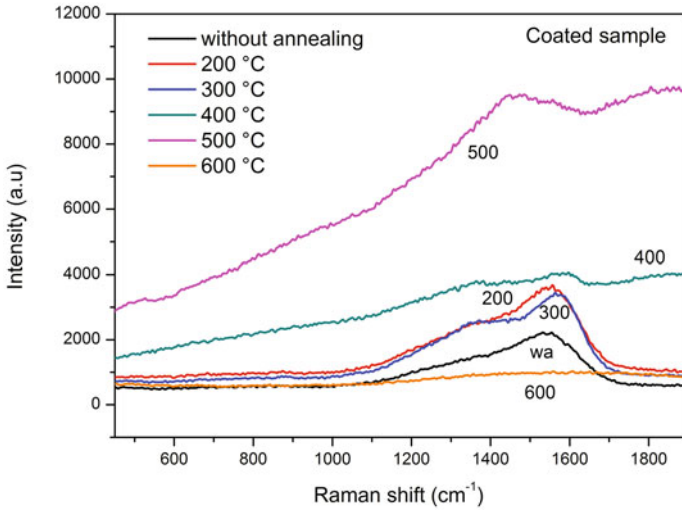


Fig. 6 Raman spectrum of coated sample for annealing at different temperatures

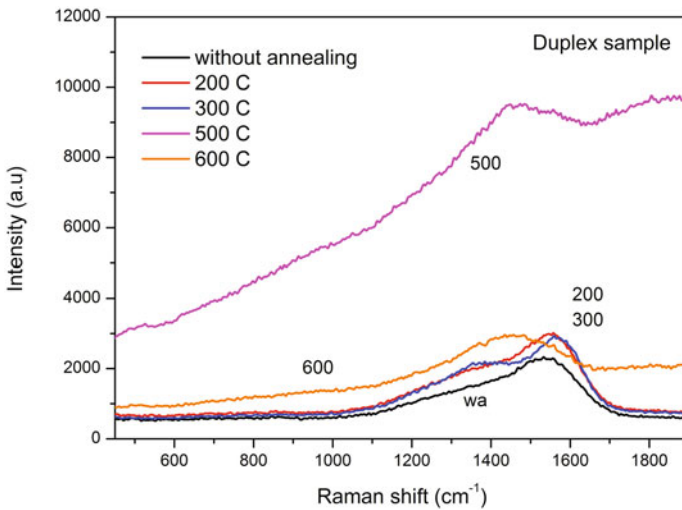


Fig. 7 Raman spectrum of duplex sample for annealing at different temperatures

Without annealing the Raman spectrum presented two overlapping bands known as the D and G bands, which were well positioned, indicating a good quality film as it was mentioned above (Fig. 2).

With annealing at 200 °C, a slight D peak position shift can be observed, and at 300 °C, it can be said that the film starts to transform (sp^3 to sp^2).

At 400 °C, a very strong fluorescence appears indicating a degradation of the diamond-like structural properties of the films.

At 500 °C, there is no DLC coating structure at all and the graphite-like component increases. A small band in the region of 500 cm^{-1} can also be detected which could correspond to the silicon interlayer.

At 600 °C, this transformation effect is more evident and the graphite band appears to be displaced.

With respect to the changes on the coating surface, a change could be observed after the annealing process at 600 °C in the duplex sample as it can be seen in Fig. 8. Large cracks were produced but there was not detachment of the coating.

In the coated sample, different features could be detected. The transformation of the coating could be observed at lower temperature, 400 °C (Fig. 9), where part of the coating was detached. After annealing at 600 °C, the transformation was completed and some cracks appeared on the surface.

According to the results of hardness and the surface images, it could be concluded that in the duplex sample the transformation of the DLC coating was produced at a higher temperature (about 600 °C) than in the coated sample. In fact, the change of color is a sign of coating degradation, the zone where the coating was vanished is observed in red.

Taking into account the Raman spectra, degradation of the coatings was detected in both samples, but probably the rate of graphitization in the duplex coating sample was lower than in the coated sample and consequently the effect of the transformation was less noticeable and it did not have any influence on the coating properties.

The adhesion was better in the duplex sample than in the coated sample. This could be due to the difference between the elastic moduli. This difference is smaller between the coating and the nitrided layer than between the coating and the stainless steel. Consequently, the stress gradient is lower, and the coating was not detached in the duplex sample.

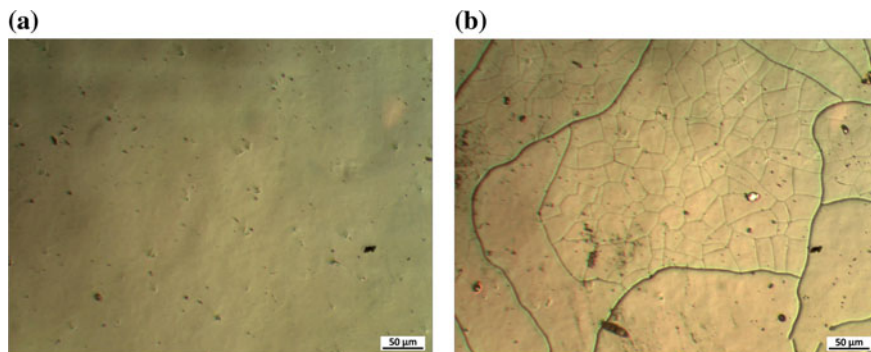


Fig. 8 Optical micrograph of duplex sample, with annealing: **a** at 400 °C, **b** at 600 °C

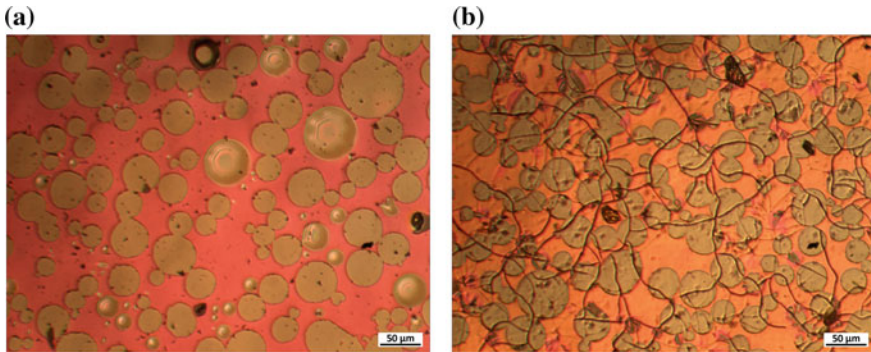


Fig. 9 Optical micrograph of coated sample, with annealing: **a** at 400 °C, **b** at 600 °C

On the other hand, during the annealing, thermal stresses are induced. Probably, these stresses were higher in the coated sample than in the duplex sample because of the presence of the silicon layer (with thermal coefficient similar to DLC) and the nitrided layer that modifies the thermal coefficient compared to stainless steel without any treatment [12, 13]. Moreover, in this sample, as there is chemical affinity between silicon of the interlayer and nitrogen of the nitrided layer, the silicon reacts with the nitrogen forming SiN as it was detected by XPS analyses, which were made by some of the authors recently. The presence of silicon nitride reduces the thermal stresses since its thermal expansion coefficient is close to the silicon thermal expansion coefficient of the interlayer [14–16].

Conclusion

The DLC coating deposited over nitrided PH steel presented better thermal stability than the same coating over stainless steel without treatment. In the duplex sample, the hardness did not decrease, the morphology of the surface did not change until 600 °C and the coating did not detach. This could be due to following: (i) the duplex samples had better adhesion, (ii) the similarity of the thermal coefficients of the nitrided layer and the DLC coating during the thermal treatment.

Acknowledgements The authors would like to thank to research scholars of GIS group (UTN) for their help in preparing of samples and tests.

References

1. Li, H., Xu, T., Wang, C., Chen, J., Zhou, H., & Liu, H. (2006). Annealing effect on the structure, mechanical and tribological properties of hydrogenated diamond-like carbon films. *Thin Solid Films*, *515*, 2153–2160.
2. Zou, Y. S., Wu, Y. F., Huang, R. F., Sun, C., & Wen, L. S. (2009). Mechanical properties and thermal stability of nitrogen incorporated diamond-like carbon films. *Vacuum*, *83*, 1406–1410.
3. Zhang, S., Bui, X. L., & Li, X. (2006). Thermal stability and oxidation properties of magnetron sputtered diamond-like carbon and its nanocomposite coatings. *Diamond and Related Materials*, *15*, 972–976.
4. Choi, H. W., Gage, D. M., Dauskardt, R. H., Lee, K.-R., & Oh, K. H. (2009). Effects of thermal annealing and Si incorporation on bonding structure and fracture properties of diamond-like carbon films. *Diamond and Related Materials*, *18*, 615–619.
5. Er, K., & So, M. (2010). Thermal annealing behavior of Si-doped diamond like-carbon films deposited by reactive sputtering. *Journal of Ceramic Processing Research*, *11*, 760–764.
6. Borges, C. F. M., Pfender, E., & Heberlein, J. (2001). Influence of nitrided and carbonitrided interlayers on enhanced nucleation of diamond on stainless steel 304. *Diamond and Related Materials*, *10*, 1983–1990.
7. Trava-Airoldi, V. J., Bonetti, L. F., Fernandes, J. A., Blando, E., Hübler, R., Radia, P. A., et al. (2007). DLC film properties obtained by a low cost and modified pulsed-DC discharge. *Thin Solid Films*, *516*, 272–276.
8. Choi, J., Soejima, K., Kato, T., Kawaguchi, M., & Lee, W. (2012). Nitriding of high speed steel by bipolar PBII for improvement in adhesion strength of DLC films. *Nuclear Instruments and Methods in Physics Research, Section B: Beam Interactions with Materials and Atoms*, *272*, 357–360.
9. Casiraghi, C., Ferrari, A. C., & Robertson, J. (2005). Raman spectroscopy of hydrogenated amorphous carbons. *Physical Review B*, *72*, 1–13.
10. Ferrari, A. C., & Robertson, J. (2000). Interpretation of Raman spectra of disordered and amorphous carbon. *Physical Review B*, *61*, 14095–14107.
11. Dalibón, E. L., Trava-Airoldi, V., Pereira, L. A., Cabo, A., & Brühl, S. P. (2014). Evaluation of the mechanical behaviour of a DLC film on plasma nitrided AISI 420 with different surface finishing. *Surface and Coatings Technology*, *255*, 22–27.
12. Li, X.-Y., Sun, Y., & Bell, T. (1999). Stability of nitrogen S-phase in austenitic stainless steel. *Materials Research Advance*, *90*, 901–990.
13. Wei, Ch., & Yen, J.-Y. (2007). Effect of film thickness and interlayer on the adhesion strength of diamond like carbon films on different substrate. *Diamond and Related Materials*, *16*, 1325–1330.
14. Azzi, M., Amirault, P., Paquette, M., Klemberg-Sapieha, J. E., & Martinu, L. (2010). Corrosion performance and mechanical stability of 316L/DLC coating system: Role of interlayers. *Surface and Coatings Technology*, *204*, 3986–3994.
15. Chen, C. W., Huang, C. C., Lina, Y. Y., Chen, L. C., & Chen, K. H. (2005). The affinity of Si–N and Si–C bonding in amorphous silicon carbon nitride (a-SiCN) thin film. *Diamond and Related Materials*, *14*, 1126–1130.
16. Tien, C. L., & Lin, T. W. (2012). Thermal expansion coefficient and thermomechanical properties of SiN(x) thin films prepared by plasma-enhanced chemical vapor deposition. *Applied Optics*, *51*, 7229–7235.